

4 JET Studies

4.1 INTRODUCTION

JET has been in shutdown for the whole of the year to install the ITER-Like Wall (ILW) and to complete the major neutral beam enhancement and a suite of diagnostic changes and improvements. The science team has concentrated on analysing and interpreting results from the experimental campaigns before the shutdown, in particular to prepare for operation with the new wall. There has also been an intense effort to develop ideas and proposals for the upcoming campaigns. Staff from all EURATOM fusion Associations work together in the EFDA JET Task Force system; in what follows we emphasise work where CCFE has had a strong contribution.

The ILW will transform the operation of JET. The carbon (carbon-fibre-composite) plasma facing components have all been replaced, with beryllium for the main part of the vessel and tungsten for the divertor. This mimics the material mix planned for the deuterium-tritium (DT) phase of ITER and may also lead to ITER starting with a tungsten divertor rather than the present plan of a combined tungsten and CFC armour, potentially saving one divertor change. One of the major motivations for the metal wall is to reduce the retention of tritium trapped in the vessel components or in co-deposits (tritium retention is a key constraint on the ITER operation regime). However, unlike carbon, metals melt, and thus the power flux to the plasma facing surfaces has to be limited, leading to special requirements on the edge and divertor plasma. It is planned to develop new high performance plasmas on JET compatible with the metal wall, and test these with tritium in a few years time.

This brief summary covers:

- Scenarios with low power flux to the divertor targets;
- Development of high performance scenarios;
- Disruption studies for ITER;
- Other studies (fast particle physics, ELMs, pellets, RF power coupling);
- Enhancement projects;
- Preparation of the ITER-like Wall campaigns.

4 JET Studies

4.2 SCENARIOS WITH LOW POWER FLUX TO THE DIVERTOR TARGETS

The high power plasmas on JET, as on ITER, have the capability to melt the metal divertor tiles, even if they are made of tungsten with its high melting point and good thermal conductivity. In JET the tungsten is either bulk (target tiles built from precisely aligned and mounted tungsten lamellae) or thin coatings on CFC tiles. This means that special plasma scenarios have to be developed with low power flux at the divertor targets and this has been a focus of the work over recent campaigns. In addition although it is difficult to sputter tungsten atoms from the surfaces, if it is sputtered and enters the plasma (a) the target is eroded and (b) the plasma can be cooled by the extra radiative losses in the core.

Therefore we need to develop plasmas where the power exhausted from the plasma is spread over the largest possible area and the temperature at the target is as low as possible. There are four main techniques available for this:

- Flux expansion (expanding the field lines – the MAST Upgrade Super-X divertor is an extreme example of this);
- Strikepoint sweeping – moving the high heat flux area over a wide region or several tiles;
- Radiative divertor – seeding the divertor plasma with impurities that radiate energy, thus spreading the power over a much larger area and also cooling the plasma to reduce the sputtering;
- Detached divertor – strong fuelling of the divertor with deuterium and or impurities to raise the density and cool the region near the divertor targets so the temperature drops to a very low level ($\sim 1\text{eV}$) and essentially no power is transferred to the targets, it is all lost by radiation or charge exchange losses.

All of these methods are used on JET. The emphasis in the last campaigns has been on the development of a radiative and/or detached divertor. In addition to the steady power on the divertor, there are pulses from events such as ELMs. On JET these are generally not large enough to cause melting, but may cause sputtering.

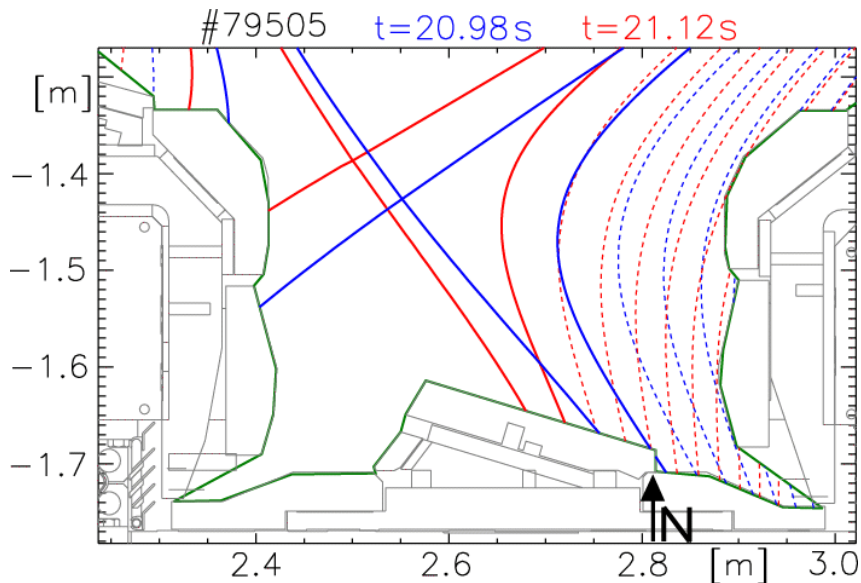


Figure 4.1: Typical magnetic equilibrium in the divertor, showing how the strike-point can be swept (red and blue show extremes) and the location of nitrogen seeding inlet (neon seeding is on the inboard side at ~2.5m).

Figure 4.1 shows the layout and location of nitrogen and neon seed impurity injection (often used in conjunction with increased puffing of deuterium). The impact on the average power was described in the 2009/10 report illustrating that it is indeed possible to greatly reduce the power flux between ELMs, and more detailed work has been done since to document the study more completely and improve our understanding of how it works, and to what extent a cold divertor is compatible with good core plasma performance. Figure 4.2 shows the effect on the power deposition profile measured with a high resolution infra-red camera. The total power is reduced, but in particular the peak power drops dramatically. Estimates of the plasma temperature show that it too is much reduced, and this reduces the sputtering of tungsten. The goal is a combination of low power flux and low temperature (down to a few eV) – this means a “detached” or partially detached plasma where the bulk of the power is radiated from the divertor plasma, not conducted to the target plates.

Divertor fuelling and seeding reduces the inter-ELM power dramatically and gives good prospects for handling very high power plasmas without damaging the ITER-like Wall. However often there is only modest reduction in the heat pulse from ELMs. Therefore radiative divertors will need to be combined on ITER with techniques to mitigate ELMs, such as external coils (simple ones exist on JET, and there is a comprehensive set on MAST), vertical “kicks” to trigger ELMs early (and keep them small) and tuning the plasma shape and scenario to find small-ELM even ELM-less regimes. These approaches will be important parts of future JET campaigns.

Most of the results described have used pre-programmed seeding of impurities. In future it will be necessary to use feedback control, possibly combined with sweeping of the strike-point across the divertor target to spread the power and energy deposited. This has

been explored and developed and Figure 4.3 gives an example. Here light emitted by seeded nitrogen has been used in a feedback loop to control the gas input. Sweeping has also been used, and the figure shows these have been combined to sustain reduced power load between ELMs.

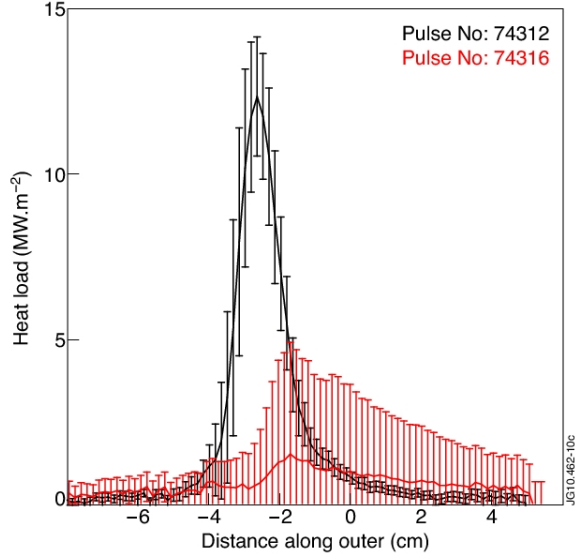


Figure 4.2: Use of neon seeding to reduce the power at the outer divertor target, measured with infra-red camera between ELMs, the solid lines showing the effect clearly. Black: reference discharge #74312. Red: seeded discharge #74316 ($D_2: 2.63 \times 10^{22}$ e/s, Ne: 0.16×10^{22} e/s)..

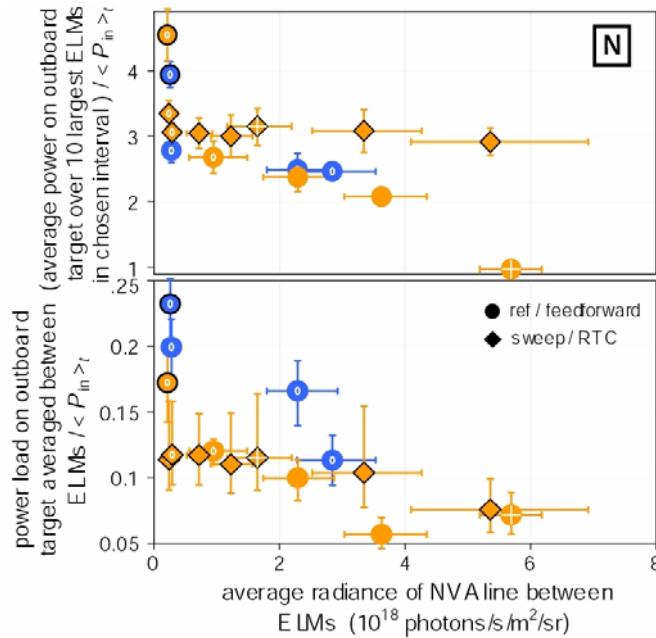


Figure 4.3: Comparison of sweeping and feedback control of the seeding (black-outlined circles & diamonds) with unswept feed-forward counterparts (circles). The horizontal axis is the nitrogen light level. Points colour-coded according to their D-fuelling level, those labeled “0” with no direct N input. Top: power landing on the whole outboard target averaged over the 10 largest ELMs in each chosen flat-top window, normalised by total input power. Bottom: average power landing on the outboard target between ELMs, normalised by total input power.

4.3 DEVELOPMENT OF HIGH PERFORMANCE AND ADVANCED SCENARIOS

ITER has two prime objectives: achieving $Q=10$ (i.e. fusion power ten times heating power) for sustained but modest pulse length (few 100 seconds), and also generating very long pulses (1000s of seconds) for technology testing and preparing for DEMO which has to have many hour or continuous plasmas. The $Q=10$ target should be attainable with standard H-mode, but there are some uncertainties (e.g. pedestal height, below). Therefore there is benefit in developing improved scenarios, building on the H-mode. These are variously called Hybrid, Improved H-mode and Advanced Inductive scenarios, and seek ways of having improved core performance, usually by tailoring the plasma current profile. For the later phases of ITER with extremely long pulses, more advanced scenarios are probably needed: these Advanced Tokamak plasmas aim to combine improved confinement, stability and current drive capabilities into a self-consistent plasma scenario.

JET Hybrid plasmas can achieve improved confinement compared with the empirical scaling for the standard H-mode by optimising the plasma boundary shape to maximise the edge stability and avoid contact with the vessel wall, and by shaping the plasma current profile to maximise the core stability. Since the fusion power depends on both density and temperature in the centre of the plasma, better performance is achieved by peaking the profiles, i.e. increasing the ratio of core to pedestal value of density, temperature or both. Furthermore recent work to project the performance of JET Hybrid plasmas to a possible future experiment with mixed deuterium and tritium fuel has highlighted the need to control the density in order to maximise the potential fusion gain.

Recent data analysis has shown that density (collisionality) and the triangularity of the plasma shape (ITER can have high triangularity) may both play key roles in determining the peaking of the temperature and density profiles of such plasmas, with higher triangularity allowing an increase in the height of the density pedestal and lower triangularity leading to an increase in the ion temperature peaking at lower collisionality. These detailed studies will provide important guidance and tools for both the design of JET deuterium-tritium experiments and the development of scenarios for ITER.

To develop Advanced Tokamak plasmas, experiments have been performed at JET for several years to investigate the prospects of combining the benefits of the high edge pressure possible with triangular plasmas and the increased core pressure peaking possible using Internal Transport Barriers (ITBs). ITBs can be generated by improving the confinement of the plasma locally in the core by modifying the current profile shape and making the core plasma rotate rapidly. But if the confinement is improved too much, the large local pressure gradient at the ITB can lead to plasma instabilities. To avoid this problem, 'weak' ITBs have been developed which only

result in a modest increase in the local pressure gradient. An example is shown in Figure 4.4.

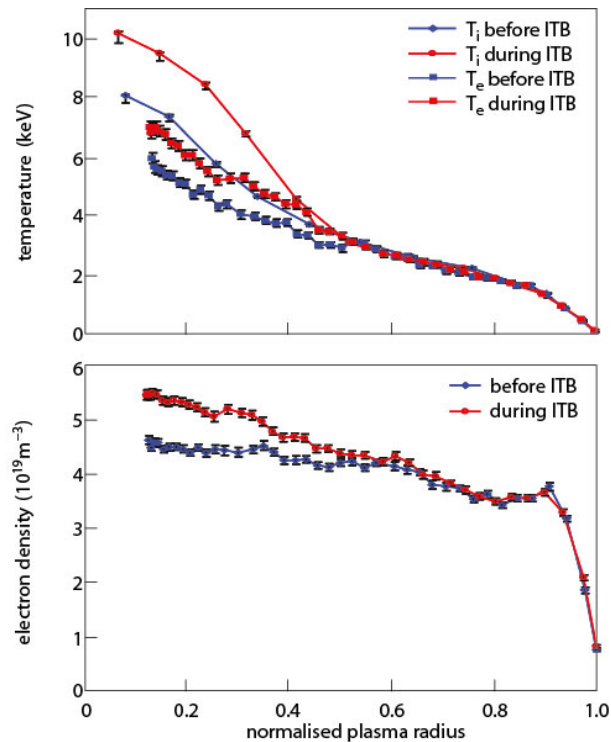


Figure 4.4: Temperature and density profiles before (blue) and after (red) the formation of a 'weak' ITB in a JET Advanced Tokamak experiment (pulse #77592).

Recent analysis of these experiments has shown that it is possible to increase the overall plasma confinement compared with the empirical scaling for the standard H-mode without generating pressure profile over-peaking. Figure 4.5 shows that the confinement relative to the standard ELMy H-mode scaling increases significantly as the ion temperature gradient at the ITB increases up to $\sim 50\%$ above the threshold level for identification of an ITB, i.e. before over-peaking.

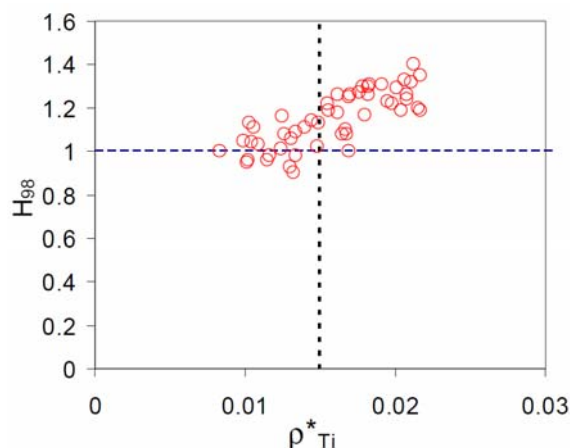


Figure 4.5: Energy confinement relative to the standard ELMy H-mode scaling (H_{98}) versus normalised ion temperature gradient in the plasma core ($\rho^* T_i = \rho_s / L_{Ti}$). The vertical line represents an empirical threshold for the temperature gradient to signify the presence of an ITB.

4.4 EDGE PEDESTAL STUDIES

The performance of ITER in the baseline ELMy H-mode regime depends on the height of the edge pedestal: the core temperature has to be in the region of 10keV, and for the H-mode regime, the transport limits the temperature gradient, thus linking the core temperature to the temperature at the top of the edge pedestal (but note the peaking discussion in section 4.3 above). Over several years extensive studies have been made on JET, DIII-D and ASDEX Upgrade to improve understanding on how the pedestal scales towards ITER. Over the last year this has become even more detailed, looking at both the density and temperature pedestals: they are not a priori identical in structure and seen to differ in experiment. In particular the measurements have been re-examined as they are at the limits of the instrumental spatial resolution – this is illustrated in Figure 4.6.

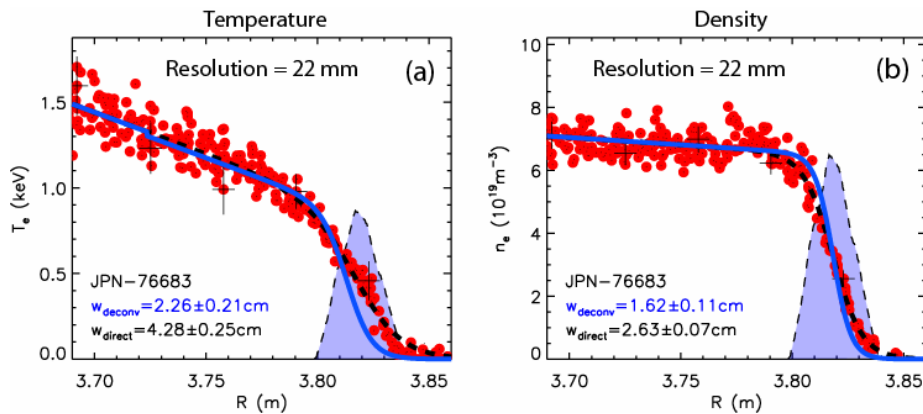


Figure 4.6: Example temperature and density pedestal measurements on JET using plasma movements to increase the effective number of spatial channels of the Thomson scattering system. The basic instrumental resolution is shown via the instrument kernel (blue shaded area). The blue curve shows the effect of deconvolving the kernel from the raw data (red points) in obtaining a better estimate of the pedestal width.

There is a limit to the maximum gradient within the pedestal, so the achievable height is related to the width. It is therefore important to see how the width scales towards ITER. One of the parameters that changes between present machines and ITER is the normalised Larmor radius (ρ^*). Figure 4.7 shows the results of careful scans on JET and on the US tokamak DIII-D which indicate the pedestal on ITER will not be significantly narrower (as a fraction of the plasma radius).

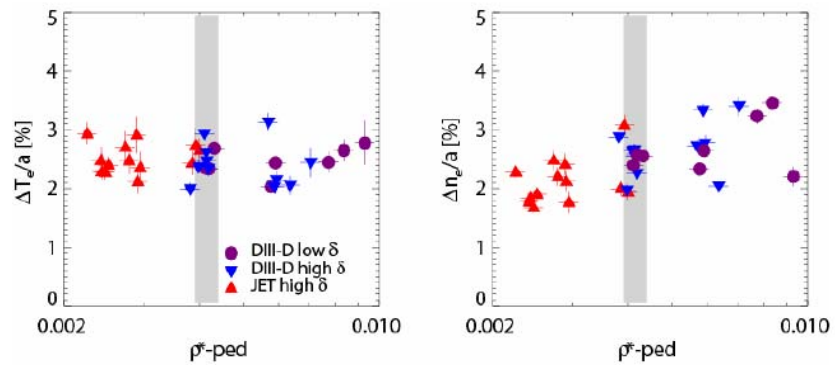


Figure 4.7: Pedestal structure parameters for JET and DIII-D as a function of ρ^* : (a) Electron temperature pedestal width from the *mtanh* fit in the outer midplane normalised to the minor radius. (b) electron density width from the *mtanh* fit. “*mtanh*” is a standard functional shape fitted to the profiles.

4.5 DISRUPTION STUDIES FOR ITER

There will be intense efforts to avoid disruptions on ITER, but there will inevitably be some, and the vessel and internal structures are being designed to withstand them. This follows many years of studies. One relatively new aspect is the issue of oscillatory rotating asymmetries and sideways forces (see Figure 4.8), and in particular whether ITER has to design against the oscillation resonating with mechanical resonances of the vessel. This is ongoing research and may guide the final design of some components as well as the disruption avoidance and mitigation techniques on ITER.

The other main aspects of disruptions are the heat deposition and runaway electrons. Figure 4.9 shows the infra-red measurement capabilities on JET, and Figure 4.10 shows data on where the heat is deposited, both the plasma thermal energy and also the energy in runaway electrons generated in one discharge. This is used for the development of mitigation schemes (e.g. by massive gas injection), and to identify the areas to monitor in the ITER-Like Wall.

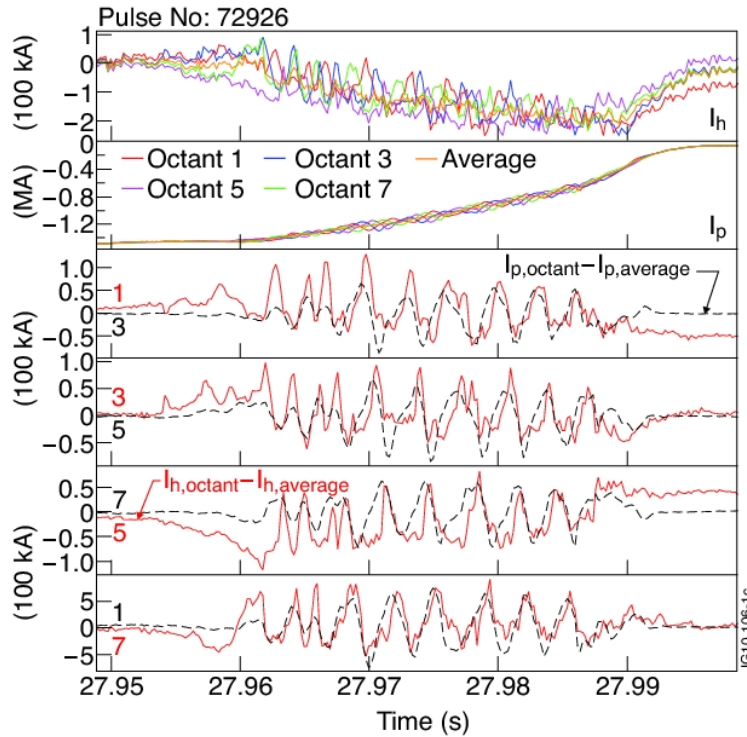


Figure 4.8: The poloidal halo current and the plasma current measured in four octants are in the top two boxes. The plasma current and TF go clockwise in JET, hence the negative sign. Negative halo current in the top of the vessel means current entering outboard and exiting inboard. The bottom four boxes have the asymmetric component of the poloidal halo current and the asymmetric component of the toroidal plasma current in each octant, with the plasma shifted toroidally by $\pi/2$.

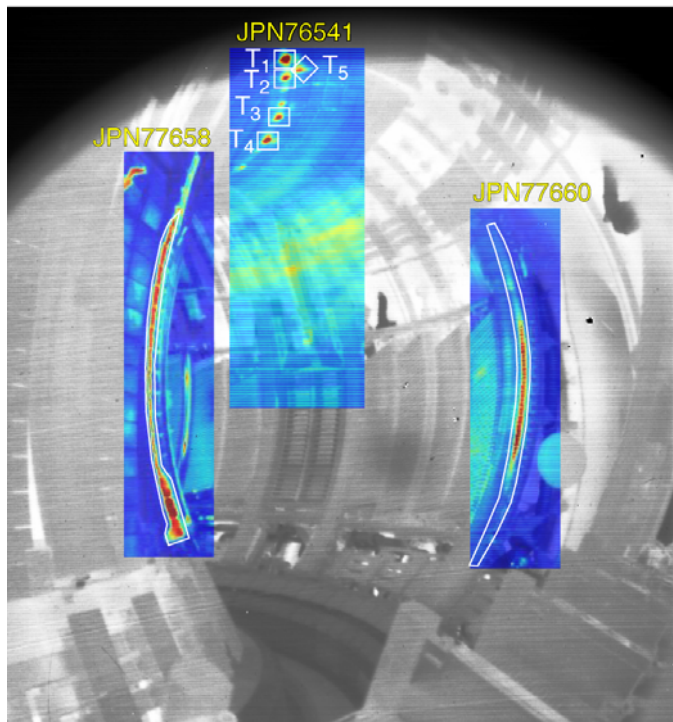


Figure 4.9: Plasma-facing components as seen by the wide angle view infrared camera. The coloured areas are examples illustrating the regions of interest selected for fast time resolution measurement (1 ms) onto key Plasma Facing Components: the upper dump plate where runaway electrons cause local hot spots (JPN 76541), the inner limiter (JPN 77658) and the outer limiter (JPN 77660).

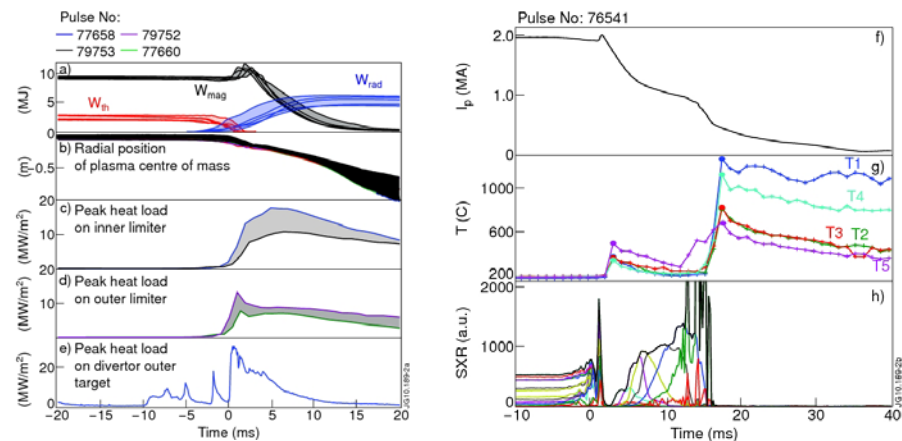


Figure 4.10: (a) the thermal (W_{th}), magnetic (W_{mag}) and radiated (W_{rad}) energies during the 40ms around the thermal quench ($t=0$). (b) the radial position of the centre of mass of the plasma with respect to the major radius, R_0 . (c) to (e) the peak heat load measured on the inner limiter, outer limiter and outer target of the divertor respectively. (f) to (g), the plasma current, I_p , and the temperatures, T_1, \dots, T_5 measured on the upper dump plate (see Figure 4.9), and (h) the soft X-ray channels, measured during a disruption with massive injection of Argon which generated a runaway electron beam ($I_{RE} = 500$ kA).

4.6 OTHER STUDIES

4.6.1 SAWTOOTH TRIGGERING OF NEOCLASSICAL TEARING MODES

ITER's performance will be improved if neoclassical tearing modes can be avoided or controlled. One of the triggers for NTMs is the sawtooth, and a recent study by a CCFE-led working group of the ITPA MHD Topical Group has examined the observation that NTMs are triggered more readily by sawteeth with longer periods (not necessarily larger amplitude). While the reason for this dependence remains unexplained, the observations are clear, and illustrated in Figure 4.11 where it is seen that the critical normalised pressure, β_N , at which a sawtooth triggers an NTM appears to decrease with increasing sawtooth period. For this and other reasons there is an effort to destabilise sawteeth so they are smaller and more frequent, for plasmas where the $q=1$ surface is present (i.e. the baseline ELMy H-mode, but not the hybrid or advanced scenarios). See also Chapter 6, section 6.2.2.2E.

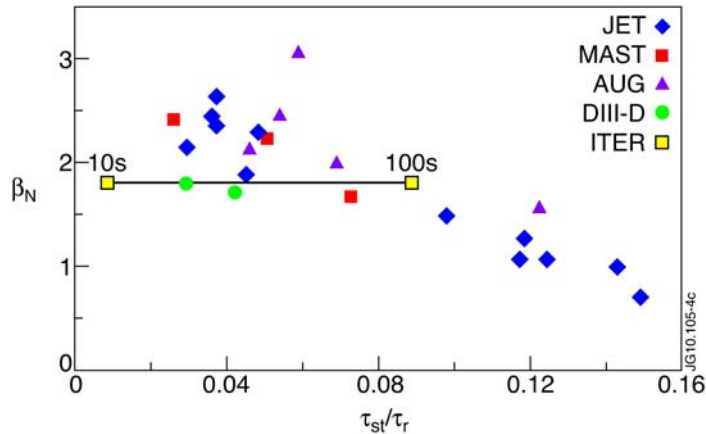


Figure 4.11: β_N at the NTM onset with respect to the sawtooth period normalized to the resistive diffusion time for ITER-like shape, $q = 1$ radius and injected power normalized to the P_{LH} threshold. For comparison, ITER Scenario 2 is indicated with sawtooth period ranging from 10 to 100 s.

4.6.2 FAST PARTICLE LOSSES

The behaviour of fast ions is important for predicting the efficiency of plasma heating by fusion alpha particles, and of current drive by neutral beam injection. This is a key part of the MAST programme as well. The scintillator probe on JET allows lost ions to be analysed according to their position in velocity space, namely their Larmor radius and pitch angle. Figure 4.12 shows an example of the losses seen before and after a magnetic reconnection event, indicating that the event has significantly depleted the confined fast ion population: the quiescent losses, assumed to be related to the confined fast ion density, are reduced after the event. Figure 4.13 shows the orbits that are sampled by the probe (whose location is shown in the figure).

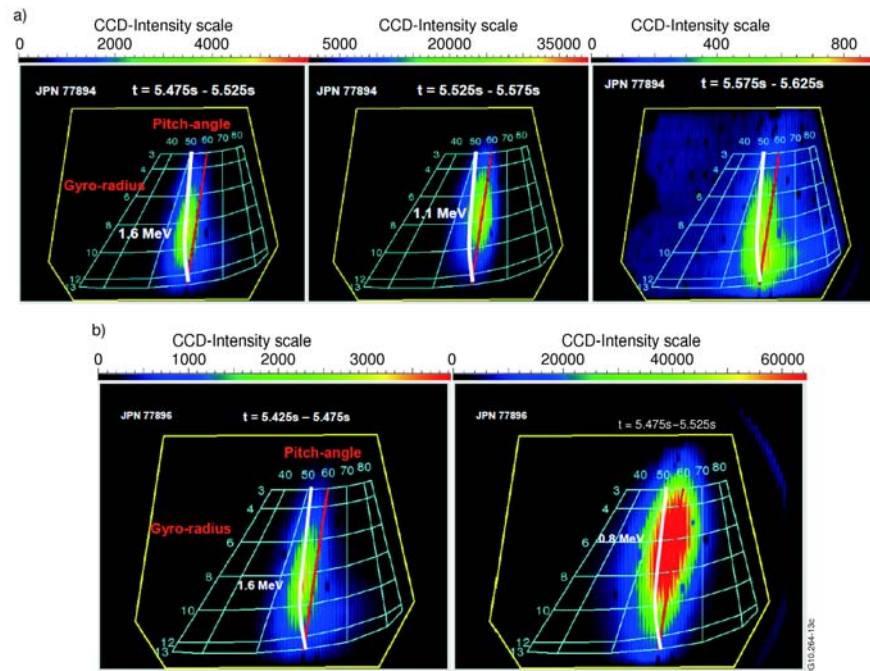


Figure 4.12: Footprints of ion losses detected with scintillator probe: (a) before during and after an internal reconnection showing reduced losses afterwards suggesting depletion of the fast ions. b) before and during a plasma disruption. The different scales are shown each 50ms frame. Red line – pitch-angle of the ICRH resonant ions; white line – the boundary between trapped and passing ions on the SP grid.

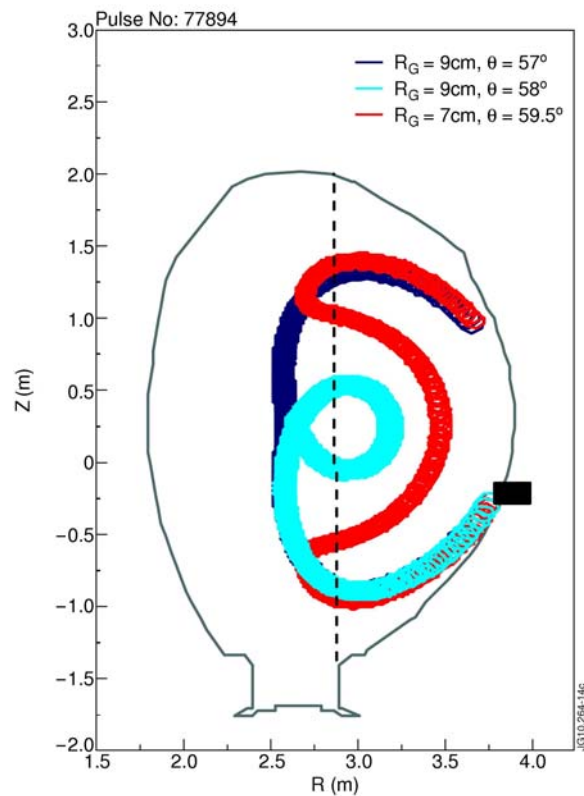


Figure 4.13: Orbits of lost H-ions calculated backward in time from (ρ, θ) coordinates on the scintillator related to the loss footprints of Figure 4.12a; dashed line – position of the ICRH resonance layer at 2.66T/1.75MA and $f_{ICRH} = 42-42.5\text{MHz}$.

4.6.3 EFFECT OF ICRH ON PLASMA FACING COMPONENTS

ITER will have a high power ion cyclotron resonance heating system (being designed by a consortium led by CCFE, Chapter 8). The high power density in front of the antenna can lead to fast ions which cause local heating or impurity sputtering from plasma facing components especially those close to the antenna (Figure 4.14). Studies on JET have made use of the co-deposited surface coatings on the septa separating the two halves of each antenna. To match the observed temperature variation, especially the cool-down when the RF is turned off, a thermal model including the thickness of the coating is needed. Figure 4.15 shows the results of this: the deduced heating flux also has to be changed as the assumed surface layer changes. The results give a measure of the power density during the RF pulse which can then be used to compare to models of the RF sheath in front of the antenna.

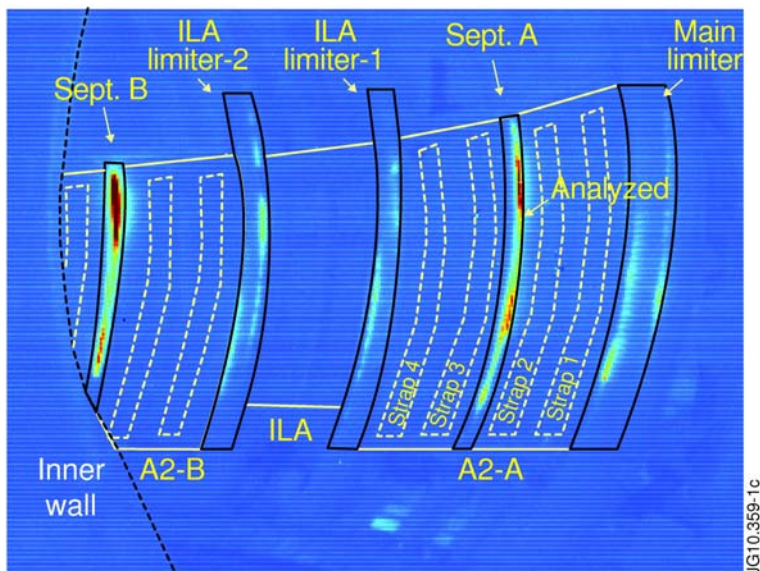


Figure 4.14: IR image, Pulse No: 79799, $t=23s$. Superimposed are the A2 antennae A and half of B, the JET ITER-like Antenna (ILA), the main and ILA poloidal limiters, and the A2 antenna septa. The location (on septum A) where analysis of the surface temperature was carried-out is shown. In this pulse, only A2 antennae A and B are used, launching 3MW.

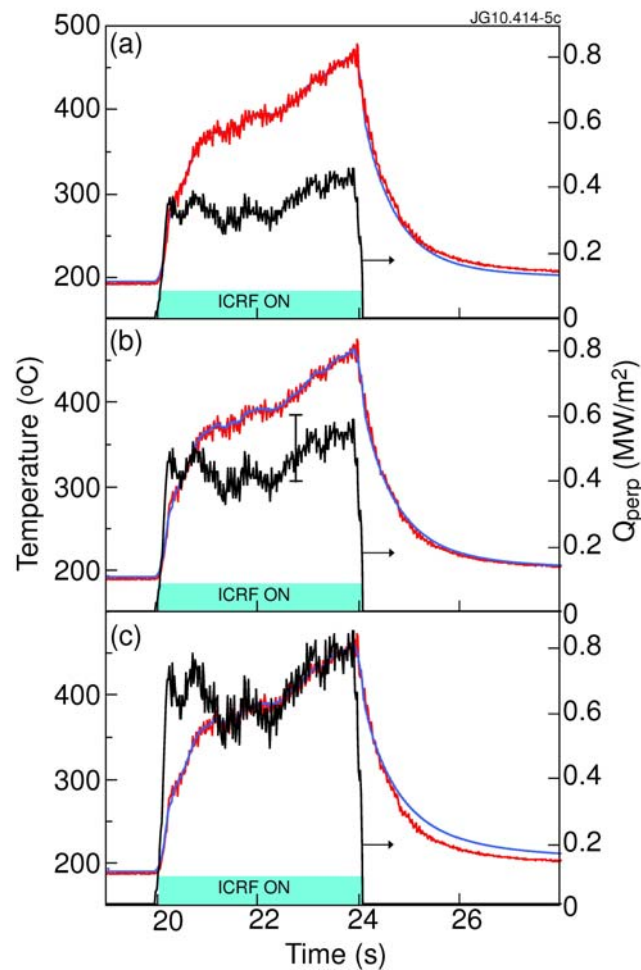


Figure 4.15: Estimate of applied heat-flux on antenna A2-A septum (at location shown on Figure 4.13), pulse #79799. The estimated flux (black curve) is on the right axis. The surface temperature, measured (red curve) or estimated (blue) is on the left axis. We imposed $Q_{\text{perp}} = 0$ for $t > 24$ s. Results are shown for the three different deposit parameters. (a) $\alpha_{\text{layer}} = 1.5 \times 10^3 \text{ Wm}^{-2} \text{ K}^{-1}$ (b) $\alpha_{\text{layer}} = 2 \times 10^3 \text{ Wm}^{-2} \text{ K}^{-1}$, (c) $\alpha_{\text{layer}} = 3 \times 10^3 \text{ Wm}^{-2} \text{ K}^{-1}$. $\tau_{\text{layer}} = 1.75$ s for all. τ_{layer} is a characteristic thermal time for the layer and α_{layer} a measure of the thermal connection to the bulk.

4.6.4 PLASMA RAMP-UP

The ramp-up phase of a tokamak plasma is often critical to attaining the optimum final state (in particular for advanced regimes including the hybrid scenario). Studies have been done to try to model this (also on MAST where similar results are found). It has generally been assumed that the plasma resistivity is well modelled by the neoclassical value (i.e. Spitzer collisional resistivity enhanced by particle trapping), and this seems to work well during the flat top. However, it does not match well in the ramp up phase, at least for some discharges. Figure 4.16 shows that the plasma seems to have a lower resistivity than expected – modelling with neoclassical resistivity produces a narrower current profile than measured. Although not yet explained, this would be helpful in generating broad profiles needed for hybrid and advanced scenarios.

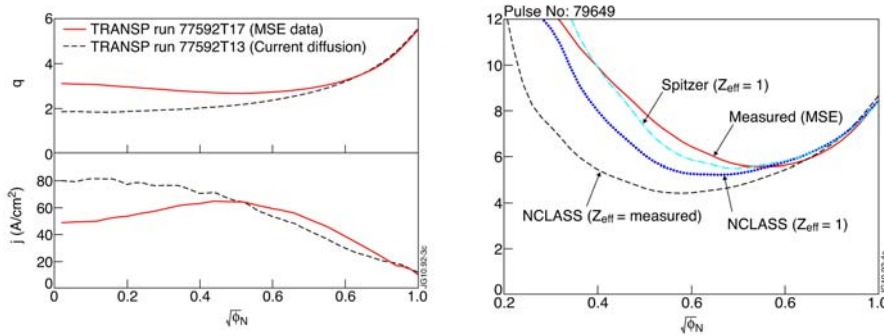


Figure 4.16: Left: comparison, at start of main heating phase, between MSE data (solid) and simulation (dashed) of q profiles and current profiles for an advanced tokamak pulse. The simulation uses a realistic initial q -profile followed by current diffusion. Right: Comparison of measured and simulated q -profiles at $t_{init}+1.4s$ for Pulse No: 79649 after 0.3s of modelled current diffusion. Z_{eff} is assumed to be flat across the plasma. ϕ_N is a measure of radius, 0 at center, 1 at edge.

4.7 ENHANCEMENT PROJECTS

CCFE has been involved in several enhancement projects as an Association, as well as its role as JET Operator (Chapter 3). The ones that were still active during 2010-2011 were:

- Neutral Beam Enhancement project (increased power and pulse length) – CCFE lead;
- Spectroscopy for the ITER-like Wall (suite of spectrometry changes to measure the new species and locations needed for the ILW exploitation phase) – CCFE leads a collaboration;
- Infra red cameras – a new project launched in 2010 to provide extra high time and space resolution of the new ITER-like Wall – CCFE leads a collaboration.

The progress on the first two is briefly described here.

4.7.1 NEUTRAL BEAM ENHANCEMENT

This very large project is now nearing completion. As is common in such projects where the engineering is close to the limit of what is achievable, some unexpected developments have appeared, but all have been overcome. The new injectors have now been tested in deuterium and helium and the overall predicted performance when various species are injected is summarised in Table 4.1.

Parameter	Gas species			
	H ₂	D ₂	T ₂	⁴ He
Max. beam energy (keV)	90	125	118	120
Max. beam current (A)	50	65	45	42
Max. power per PINI (MW)	1.0	2.16	2.2	1.56
Max. power per NIB (MW)	8.0	17.3	17.6	12.5
Max. total power (MW)	16.0	34.6	35.2	25.0

Table 4.1: Measured (D₂ and ⁴He) and predicted (H₂ and T₂) parameters of the JET NBI system after the completion of EP2 upgrade.

The actively cooled high heat flux components (mainly hypervaportrons) have all been installed. The overall power into the plasma will be increased as the programme needs, noting the requirement to avoid melting of the new metal wall, and the programme to develop suitable plasmas (section 4.2).

4.72 SPECTROSCOPY FOR THE ITER-LIKE WALL

This project is also nearing completion. All the equipment has been procured (in particular bespoke spectrometers and new, faster, higher efficiency CCD cameras for the spectrometers) a new spectroscopy lab has been created and the DT-compatible wide-band imaging spectrometers looking at the new tungsten divertor have been replaced, with completely rebuilt and improved optics. A major activity this year has been the absolute end-to-end calibration of the systems, using a dedicated broad band source (an integrating sphere) inside the vessel, using remote handling.

4.8 PREPARATION FOR THE ITER-LIKE WALL CAMPAIGNS

New task forces (E1 and E2) were set up in 2009 to start to prepare for the campaigns, now due to start in late summer 2011; three of the eight task force leaders and deputies are from CCFE. A long process involving numerous working groups, two General Planning Meetings and wide involvement of all the EURATOM Associations culminated in a call for participation of working groups in February 2011. CCFE submitted a wide ranging response, seeking leadership for many of the experiments. In addition there has been first preparation of the case for a tritium and D-T campaign, which may take place around 2015 if approved, in which CCFE would expect to play a strong role, both in plasma science and the operation (especially tritium aspects).